Fast Diffusion and Void Formation in a Two-Segment Copper-Tin Lead-Free Nanowire System with One-Dimensional Confinement

Fan Gao[1], Zhenyu Liu[2], Guangwen Zhou[3], Judith C. Yang[2], and Zhiyong Gu[1,*]

[1]*Department of Chemical Engineering, University of Massachusetts Lowell, Lowell, MA 01854, USA*
[2]*Department of Chemical and Petroleum Engineering, University of Pittsburgh, Pittsburgh, PA 15261, USA*
[3]*Department of Mechanical Engineering, Binghamton University, State University of New York (SUNY),*
Binghamton, NY 13902-6000, USA

ABSTRACT

We present experimental observations of electron-beam irradiation induced diffusion and void formation confined in a one-dimensional two-segment copper-tin (Cu–Sn) nanowire system. The two segmented Cu–Sn nanowires were synthesized by a layer-by-layer electrodeposition method using a nanoporous template. The structure and morphology of the nanowires were characterized by SEM, STEM, TEM, EDS and elemental mapping. Under e-beam irradiation, it is found that the nanowire surface oxide effectively confined the movement of metallic copper and tin atoms and the void regions were formed due to anisotropic diffusion rates and/or Sn melting. It is also seen that Cu/Sn alloy nanoparticles were formed on the oxide layer in the void regions. Such 1-D cylindrical nanowire structure presents an ideal system for understanding dimensionally confined transport phenomena and alloy formation at the nanometer scale.

KEYWORDS: Nanowires, Lead-Free Solders, Copper-Tin, Diffusion, Nanoelectronics Assembly.

1. INTRODUCTION

Soldering is widely used in electronics assembly and packaging. Recently, due to the environmental and health concerns of lead, traditional tin-lead (Sn-Pb) solders are being phased out and lead-free solders are becoming increasingly popular. Furthermore, the demand for high-performance interconnects in advanced packaging has caused the dramatic scaling down of the electronics packaging feature size from microscale to nanoscale. Among several techniques that have been proposed to address the nanoscale assembly and packaging, nanosolder-based joining and interconnection techniques provide great potential for forming robust joints between nanostructures and integrating nanocomponents into a functional device or complex system.[1–3] In order to meet the green manufacturing requirements, nano-soldering based on lead-free solder materials would certainly hold greatest advantage. However, many fundamental issues involving nano-soldering have not been addressed, such as surface wetting on various substrates, diffusion, intermetallic formation, nanojoint

strength and reliability, etc. The lack of understanding in these important issues hinders the development of this promising nano-joining technique. In many conventional applications involving copper-based circuitry, the interdiffusion between solder and copper substrate has been studied extensively for its significant role in Cu–Sn intermetallic formation.[4–6] However, the diffusion and resulting structure evolution in nanoscale Cu–Sn systems have not been studied yet. Solder nanowire is an ideal model system for studying the solder diffusion at the nanoscale.

Electron beam irradiation, due to the strong energy of electron beam, has been widely used to induce phase transformation,[7] shape transformation,[8] and structure transformation.[9] In this report, we present experimental investigation of one-dimensional diffusion in a lead-free Cu–Sn two-segment nanowire system induced by electron beam irradiation in a transmission electron microscope (TEM). Using the e-beam irradiation, rather than by the traditional heating treatment, allows us to study the local interfacial transport and reactions in individual nanowires. Our observations show that both Cu and Sn have fast interdiffusion under e-beam irradiation, which leads to void formation, called 'Kirkendall voids', near the Cu–Sn interface and around both ends of the nanowires. A diffusion and void formation mechanism is proposed based on our experimental observations.

ARTICLE
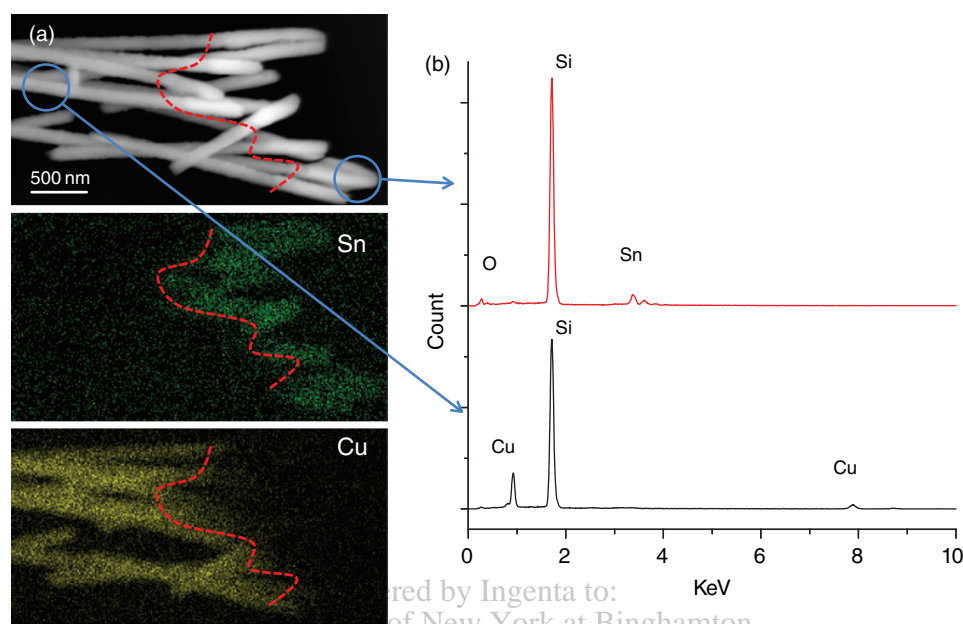
Fig. 1. (a) SEM image of as-fabricated Cu–Sn two-segment nanowires at backscattered mode and EDS mapping for each segment; (b) spot mode EDS spectra for Sn-rich segment and Cu-rich segment from Figure 1(a).

2. EXPERIMENTAL DETAILS

The Cu–Sn two-segment nanowires were fabricated by sequential layer-by-layer electrodeposition method using a polycarbonate nanoporous membrane (Whatman) at room temperature. The average diameter of the nanopores was 50 nm (nominal value). The template has a gradual diameter increase from the surface to the inside channels. Cu was deposited first using a commercial Cu plating electrolyte (Cu U-bath RTU, Technic, Inc.) with the current controlled at 2 mA/cm^2. After Cu plating, the Sn layer was electroplated by commercial Sn plating electrolyte
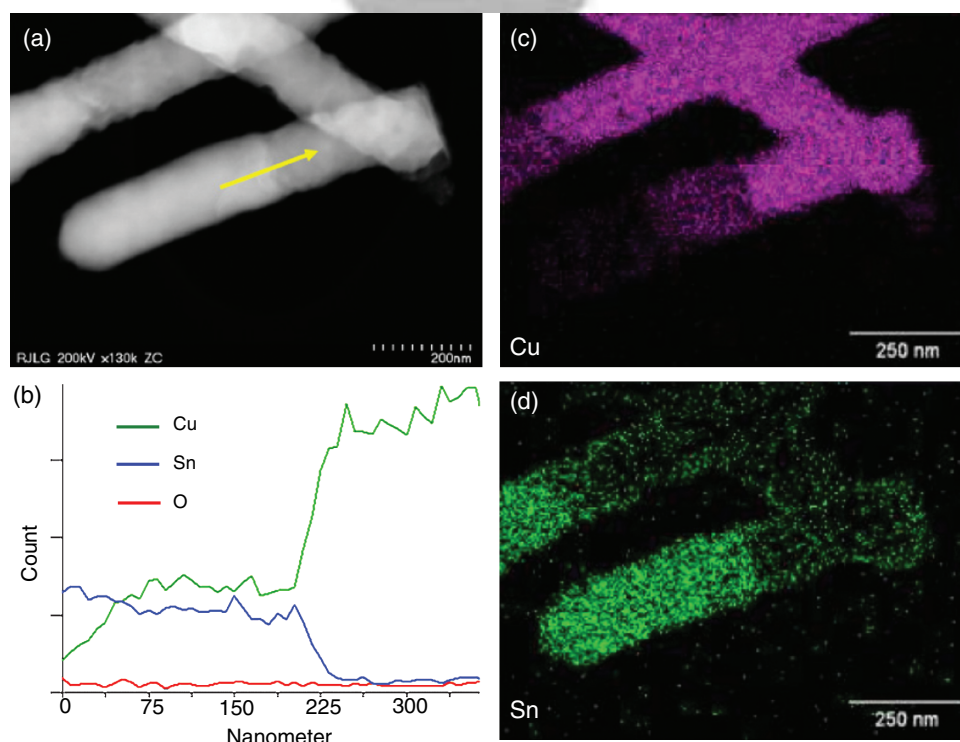
Fig. 2. (a) Z-contrast STEM image of Cu–Sn nanowires at interface; (b) line profiles of copper, tin and oxygen elements across the interface as indicated by the arrow shown in Figure 2(a); (c–d) the elemental mapping of Cu (c) and Sn (d).

(Sn Concentrate with make-up solutions, Technic, Inc.) with the current controlled at 18 mA/cm^2. After the electroplating, the polycarbonate membrane was dissolved in dichloromethane to release the nanowires into the solvent. The free-standing nanowires were cleaned and stored as a suspension in ethanol. The experimental setup and detailed information can be found from the previous publication.[10] The as fabricated Cu–Sn two segment nanowires were characterized by a JEOL-7401 field-emission scanning electron microscopy (FE-SEM) equipped with energy dispersive X-ray spectroscopy (EDS). The instrument was operated at 15 keV under backscattered mode to get better imaging contrast in different segments.

TEM samples were prepared by depositing Cu–Sn segmented nanowire samples (dispersed in ethanol) on a lacey carbon film supported on a Mo grid (SPI Supplies). A Mo grid was employed because its EDS spectrum is featureless near the Cu and Sn K, L lines used in the quantitative elemental analysis. TEM imaging and EDS spectroscopy were performed on a JEOL 2100F electron microscope equipped with an Oxford INCA 30 mm^2 atmospheric thin window (ATW) detector; the instrument was operated at 200 keV. All micrographs were acquired by a GIF TRI-DIEM post-column energy filter (Gatan Inc.) and analyzed using DigitalMicrograph (Gatan Inc.) software. Z-contrast Scanning TEM images (STEM) and EDS spectra were also obtained on a Hitachi HD-2300A.

3. RESULTS AND DISCUSSION

Cu and Sn two segments were fabricated in the form of nanowires for the diffusion couple study. Figure 1 shows SEM images of as-synthesized Cu–Sn nanowires with EDS characterization. The two segments can be clearly identified from the backscattered mode SEM image, as shown in Figure 1(a), and the red color dashed lines indicate the possible Cu–Sn interfaces from the contrast difference. The brighter segment corresponds to the Sn-rich segment which has a higher atomic number than the darker region with the Cu-rich segment. From the EDS elemental mapping image shown in Figure 1(a), it is easy to distinguish the two different elements at each location, which is consistent with contrast feature in the backscattered mode SEM image. Green and yellow areas delineated by the dashed line in the SEM image correspond to the tin and copper segments, respectively. It can be seen that the yellow signal crosses the interface with less intensity, suggesting a certain amount of copper atoms may have already migrated to the neighboring tin segment around the interfacial region during fabrication. The spot mode EDS spectra were collected from both the Cu-rich and Sn-rich segments (close to each end, as indicated by the circles in the SEM image of Fig. 1(a)). From Figure 1(b), the EDS results show that the Cu-rich segment and Sn-rich segment contain larger than 99% purity of Cu or Sn in each segment,

which confirms that there were two distinct segments. It is believed that no significant interdiffusion occurred under the low e-beam energy irradiation from the SEM. The big Si peak is from the background of the Si wafer, which was used to prepare the samples. There are two major factors that could contribute to the interface diffusion that may have occured during the electroplating process: electric field assisted ion diffusion and thermal diffusion. Since the Cu layer was deposited first, it is possible that a certain amount of top layer Cu atoms slowly diffused into the neighboring Sn layer during the tin electroplating.

The interface area was further studied through the STEM and EDS mapping. Figure 2(a) shows the Z-contrast STEM image of the Cu–Sn nanowire at the Cu–Sn interface area. Similar as Figure 1(a), the brighter contrast part represents Sn-rich segment and the darker contrast represents Cu-rich segment. There are three nanowires in the image, with one nanowire (Cu segment) lying on the top of the other two nanowires (on the Cu segments). An EDS line scan was performed across one nanowire interface as shown in Figure 2(b). An abrupt change in the Cu and Sn concentration is observed at the interface between the copper and tin segments, which is consistent with the abrupt contrast change across the interface as shown in Figure 2(a). The EDS line scan also reveals that almost
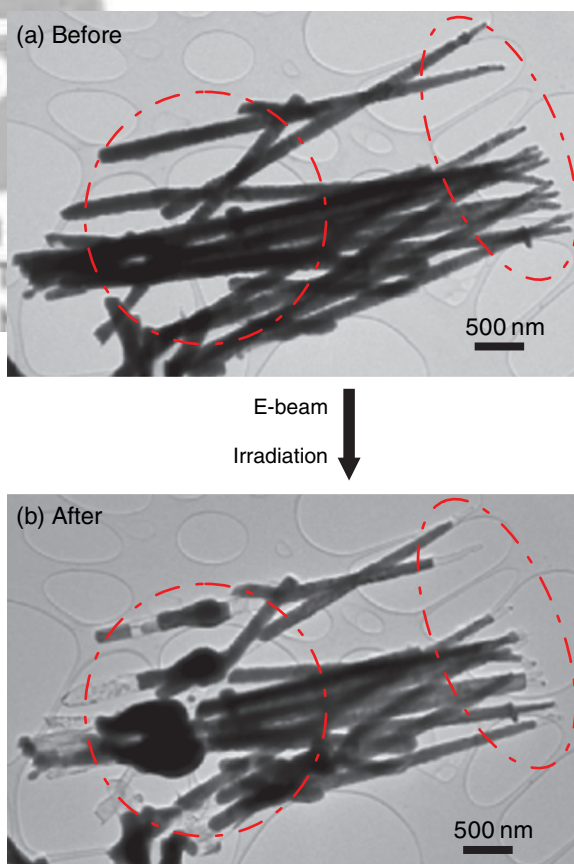

Fig. 3. TEM images showing the shape transformation of Cu–Sn two segmented nanowires (a) before and (b) after the e-beam irradiation.

no Sn was detected in the Cu segment. However, a certain amount of Cu was observed in the Sn segment, where the Cu concentration was constant for ~150 nm away from the interface, indicating the formation of a ~150 nm Cu–Sn intermetallic phase. After this interfacial layer, Cu element gradually decreases towards the end of the Sn segment. The elemental mapping of the Cu (Fig. 2(c)) and Sn (Fig. 2(d)) also reveals a ~200 nm region that contains both Cu and Sn, showing the interfacial region. However, there is no significant tin signal shown in the Cu-rich region beyond the interface, as shown in Figure 2(d). These results are consistent with SEM and EDS mapping result in Figure 1.

In order to investigate the effect of e-beam irradiation on the evolution of the mictrostructure and composition in the nanowires, several Cu–Sn nanowires suspended on the TEM grid were selected with regular imaging electron beam illumination. Figure 3 shows the morphology change of the nanowires after the e-beam irradiation. The nanowires were uniform in size before the e-beam irradiation. Due to the template limitation, the end of the Cu segment has a sharp tip (smaller diameter). After the e-beam irradiation, there were voids formed at the tips of the Cu-segments, but most copper were confined and kept in the nanowire shape. However, there was significant morphology transformation on the Sn-rich segment and big bulges formed. Large translucent voids were formed near the interface and on both Cu-rich and Sn-rich segments. These voids, called "Kirkendall void," formed because of

the difference in diffusion rates between two components in a diffusion couple.[11] With an increase in the e-beam exposure time, the void area would enlarge. The outer shell of voids is copper oxide or tin oxide which may have formed during the nanowire fabrication and storage. On the other hand, local tin melting may also contribute to the void formation around the interface. The melting of Sn under electron-beam irradiation may be caused by a temperature rise due to electron thermal spikes in the nanowire and poor thermal conduction away.[12] On the other hand, it has been reported that there is a quasi-melting phase distinct from the thermodynamic molten state existing in small particles where the particles are continuously fluctuating between different structures at temperature well below the melting point.[13, 14] Hence, although the thermodynamic melting point of Sn is as high as 232 °C, the melting under the e-beam can be observed at a relatively low temperature. This phenomenon initiated by e-beam irradiation in TEM has been reported in other systems such as Pb nanobelts,[15] ZnS nanowire,[16] etc.

A higher resolution TEM image of a representative Sn-rich region of the nanowire after the e-beam irradiation is shown in Figure 4. Most of the Sn element diffused into the Cu-rich region and a void area confined in an oxide shell was formed. The dark tip shown on the top of the Sn-rich segment was confined at the end which may be due to relative higher surface tension trapped. From the EDS data and elemental composition analysis, those dark areas around both the tip and Cu–Sn interface area were
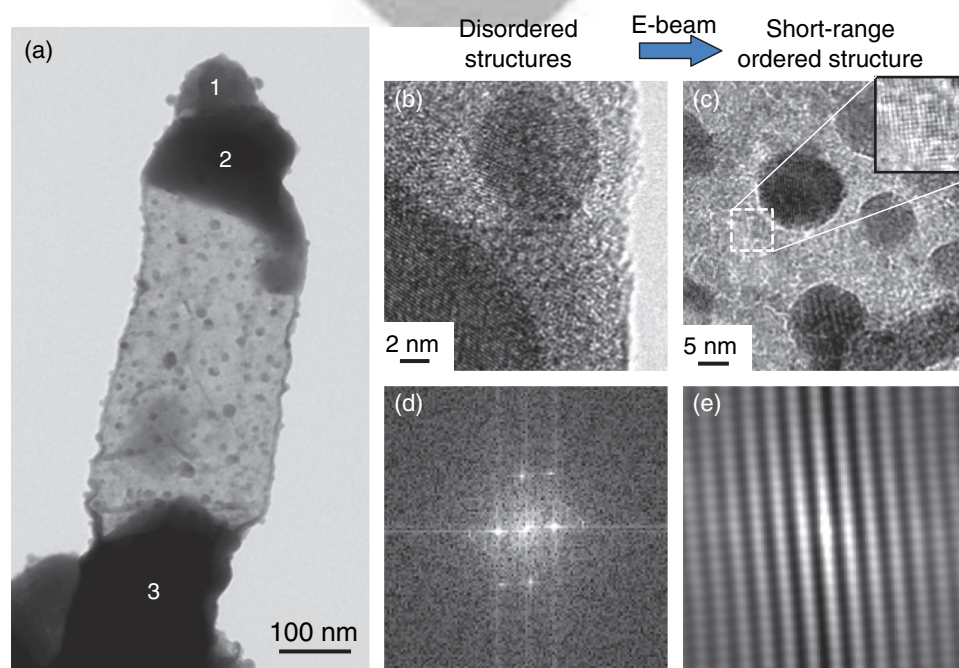
Fig. 4. (a) TEM images of Sn-rich region after e-beam irradiation; (b) HRTEM image of crystalline nanoparticles distributed on the disordered amorphous oxide shell in the void area; (c) HRTEM image of the reorganized larger crystalline nanoparticles and short-range ordered structure (inset image) formed on the oxide shell after the e-beam irradiation; (d) Fast Fourier transformed pattern of the crystalline ordered nanoparticle in (c); (e) inverse fast Fourier transform image of (d).

Table I. Composition analysis of the Sn-rich segment (Fig. 4(a)) after e-beam irradiation.

| Point	Element weight%	
	Cu	Sn
1	37.79	62.21
2	19.46	80.54
3	51.02	48.98

confirmed as Cu/Sn alloy compounds with various ratios, as shown in Table I. The large amount of Cu ratio confirmed the diffusion of Cu atoms into the Sn-rich regions under e-beam irradiation. From the corresponding HRTEM images, many nanoparticles were formed after the irradiation and were randomly distributed on the amorphous oxide shell surface. From Figures 4(b)–(c), it is interesting to observe that the nanoparticles were e-beam sensitive, since the focused nanoparticles tended to transform

into better crystalline structure after longer e-beam irradiation. Some of the amorphous area with disordered structure would also transform into short-range ordered structure which were enlarged and shown in Figure 4(c) inset. The EDS results reveal that the nanoparticles are intermetallic rather than metal oxide. It is possible that the metallic nanoparticles were formed after atomic diffusion and then e-beam reduction/re-organization.[17] Figures 4(d)–(e) are the fast Fourier transform (FFT) and inverse fast Fourier transform (IFFT) images of the crystalline nanoparticles in Figure 4(c), showing the identification of the diffraction spots.

In Figure 5, the Cu-rich region with void area was characterized by HRTEM imaging. The Cu-rich region does not show melting behavior due to its high melting point, but the atomic diffusion can be clearly observed under the e-beam irradiation as shown in both Figures 3(b) and 5(b). Figure 5(c) shows the interface region of the
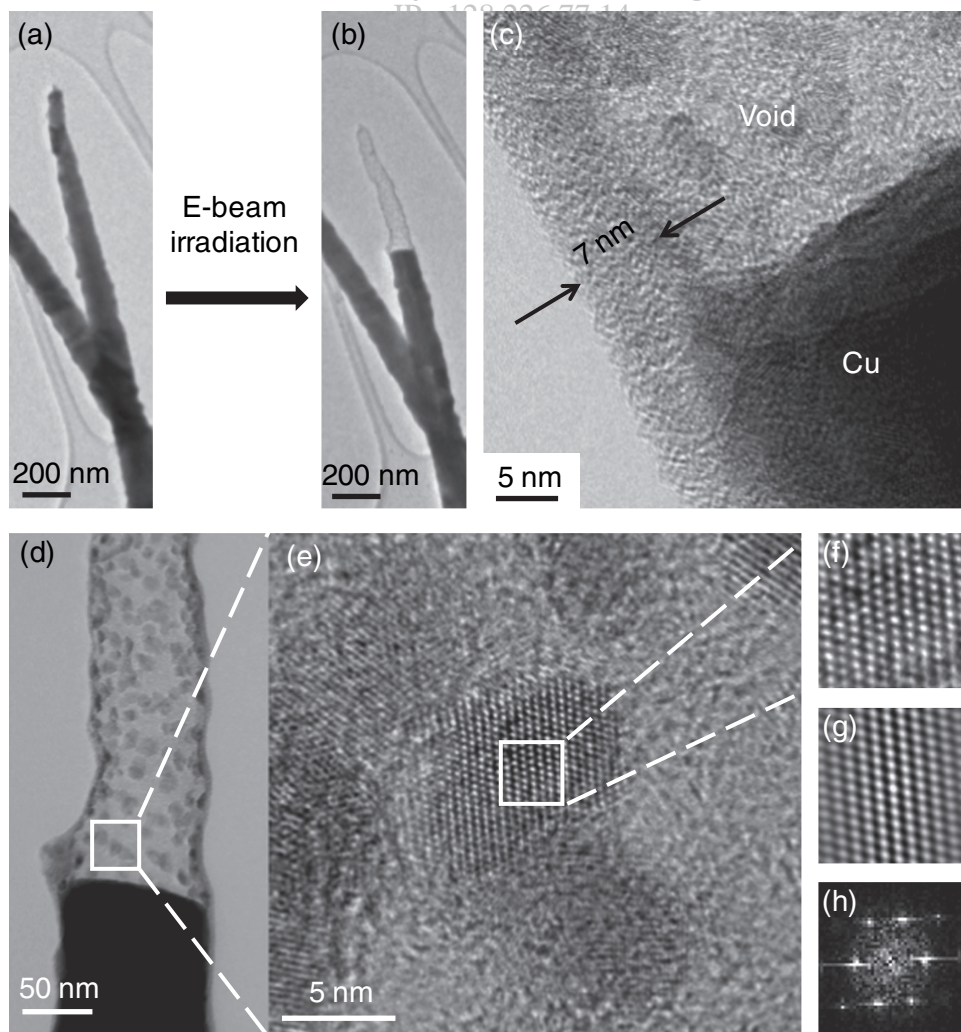
Fig. 5. TEM images of Cu-rich segment (a) before and (b) after e-beam irradiation; (c) HRTEM image of oxide shell of Cu segment with thickness measurement; (d) zoom in HRTEM image of Figure 5(b) with nanoparticles distributed on the copper oxide layer; (e) HRTEM image of crystalline ordered nanoparticles; (f) HRTEM in the selected square area in (e); (g) filtered HRTEM image of (f); (h) fast Fourier transformed image of (g).
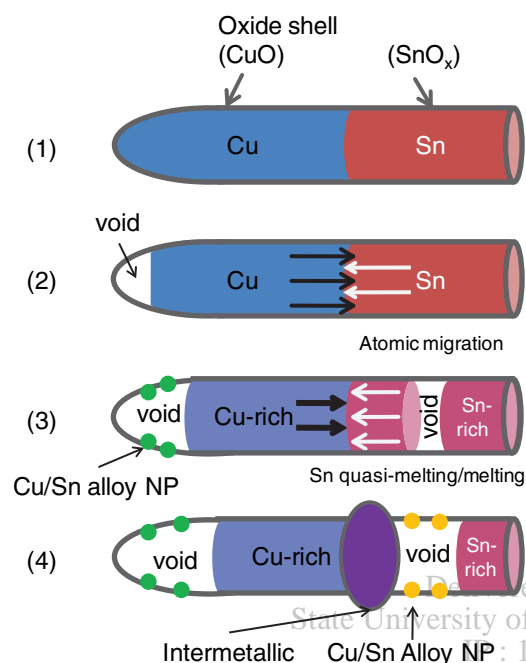
Fig. 6. Schematic of proposed diffusion and void formation mechanism. (1) original nanowire before e-beam irradiation; (2) anisotropic atomic diffusion in both Cu-rich and Sn-rich regions; (3) with the e-beam irradiation increasing, Sn-rich region reached quasi-melting/melting state with much faster diffusion into Cu-rich region along the axial direction and the void area appeared; (4) intermetallic compounds grew to prevent further diffusion between Cu and Sn.

amorphous copper oxide layer in the void area, neighboring with the metallic copper segment. Same as the Sn-rich segment, the Cu-rich segment contains an oxide layer of about 7 nm thickness which can effectively confine the Cu diffusion along the axial direction under the e-beam irradiation. Nanoparticles distributed in the void area in Figure 5(d) had variable composition, similar to those in the Sn-rich void area by corresponding EDS analysis. The HRTEM image of nanoparticles distributed on the amorphous copper oxide shell is shown in Figure 5(e) and the crystalline lattice is enlarged and shown in Figure 5(f). The Figures 5(g)–(h) are the filtered HRTEM image and FFT of squared area in Figure 5(e), which are in excellent correlation and confirms the crystal structure of the nanoparticles.

Based on experimental observations, a possible Cu–Sn diffusion and void formation mechanism is proposed as shown in Figure 6. At the beginning, due to the fact that copper has a smaller atomic size, the short time e-beam irradiation initiated fast copper diffusion into the Sn-rich region. It has been reported that the magnitude of the diffusivity of copper in tin is orders of magnitude greater than that of tin in copper,[18] which resulted in the copper atom migration and the Kirkendall void formation at the end of nanowire in the Cu-rich segment. With an increase of the e-beam exposure time, tin was activated and reached the quasi-melting/melting state. The melting

rate was much faster than the diffusion rate,[19] and thus most of tin diffused into the Cu-rich region along the axial direction under the tin oxide layer confinement and formed intermetallic compounds. Under further intensive e-beam irradiation, the Cu/Sn alloy particles were formed and distributed on the amorphous oxide shell and then reorganized to form larger particles with better crystalline structure. The amorphous area would also transform into short-range ordered crystalline structure. Once the intermetallic layer is formed, the diffusion rate will dramatically decrease and further diffusion will be prevented. From this point of view, the e-beam induced irradiation on the Cu–Sn diffusion system is consistent with the thermal treatment method.[20, 21]

4. CONCLUSION

In summary, two segmented Cu–Sn nanowires were successfully synthesized by a sequential electrodeposition method using a nanoporous template. The diffusion and void formation of Cu–Sn segmented nanowires induced by e-beam irradiation in a TEM have been studied. The metallic copper and tin embedded in the oxide shell were sensitive to the e-beam irradiation, resulting in the atomic diffusion, quasi-melting/melting of tin, and void formation. Alloy nanoparticles were formed on the oxide shell in the void regions. The diffusion was confined along the one-dimensional structure due to the thin surface oxide layer.

References and Notes

1. Z. Gu, H. Ye, D. Smirnova, D. Small, and D. H. Gracias, *Small* 2, 225 (**2006**).
2. F. Gao and Z. Gu, *Nanotechnology* 21, 115604 (**2010**).
3. Q. Cui, F. Gao, S. Mukherjee, and Z. Gu, *Small* 5, 1246 (**2009**).
4. A. Kar, M. Ghosh, A. K. Ray, and R. N. Ghosh, *Mat. Sci. Eng. A* 459, 69 (**2007**).
5. S. Li and C. Basaran, *Comp. Mater. Sci.* 47, 71 (**2009**).
6. S. Kang and A. Sarkhel, *J. Electron. Mater.* 23, 701 (**1994**).
7. X. Huang, S. Li, Y. Huang, S. Wu, X. Zhou, S. Li, C. L. Gan, F. Boey, C. A. Mirkin. and H. Zhang, *Nat. Commun.* 2, 292 (**2011**).
8. B. Wang, Y. H. Yang, and G. W. Yang, *Nanotechnology* 17, 5916 (**2006**).
9. K. H. An, K. A. Park, J. G. Heo, J. Y. Lee, K. K. Jeon, S. C. Lim, C. W. Yang, Y. S. Lee, and Y. H. Lee, *J. Am. Chem. Soc.* 125, 3057 (**2003**).
10. F. Gao, S. Mukherjee, Q. Cui, and Z. Gu, *J. Phys. Chem. C* 113, 9546 (**2009**).
11. Y. Yin, R. M. Rioux, C. K. Erdonmez, S. Hughes, G. A. Somorjai, and A. P. Alivisatos, *Science* 304, 711 (**2004**).

12. T. Yokota, M. Murayama, and J. M. Howe, *Phys. Rev. Lett.* 91, 265504 (**2003**).
13. P. M. Ajayan and L. D. Marks, *Phys. Rev. Lett.* 60, 585 (**1988**).
14. P. M. Ajayan and L. D. Marks, *Phys. Rev. Lett.* 63, 279 (**1989**).
15. Z. W. Pan, Z. R. Dai, and Z. L. Wang, *Appl. Phys. Lett.* 80, 309 (**2002**).
16. B. Liu, Y. Bando, M. Wang, C. Zhi, X. Fang, C. Tang, M. Mitome, and D. Golberg, *J. Appl. Phys.* 106, 034302 (**2009**).
17. Y. Komuro and Y. Matsumoto, *J. Phys. Chem. C* 115, 6618 (**2011**).
18. B. F. Dyson, T. R. Anthony, and D. Turnbull, *J. Appl. Phys.* 38, 3408 (**1967**).
19. M. Mouas, J. G. Gasser, S. Hellal, B. Grosdidier, A. Makradi, and S. Belouettar, *EPJ Web of Conferences* 15, 01013 (**2011**).
20. K. Zeng, R. Stierman, T.-C. Chiu, D. Edwards, K. Ano, and K. N. Tu, *J. Appl. Phys.* 97, 024508 (**2005**).
21. C.-C. Pan, C.-H. Yu, and K.-L. Lin, *Appl. Phys. Lett.* 93, 061912 (**2008**).

ARTICLE